8 Pole High Temperature Superconductor Microstrip Dual Band Bandpass Filter Design

Kenneth S. K. Yeo[1] and Michael J. Lancaster[2]

[1]School of Computing, IT and Engineering, University of East London, London E16 2RD, UK
[2]Electronic, Electrical and Computing Eng., The University of Birmingham, Birmingham B15 2TT, UK

Abstract — Dual-band filters are normally used for filtering two frequency bands that are not too close together. However, this paper presents a HTS dual-band bandpass filter that can be used to achieve isolation between two frequency bands that are only a few tens of MHz apart. Transmission zeros are placed in between the two frequency bands using electromagnetic coupling between non-adjacent resonators which result in high isolation between the two bands. The simulation and experimental results of a High Temperature Superconductor dual-band bandpass filter with very narrow bandwidth will be presented here.

***Index Terms* — Bandpass, dual-band, filter, HTS, microstrip, superconductor.**

I. Introduction

Dual-band bandpass filters have received must attention in recent years. This is mainly due to the rapid evolving wireless communication technology, and also the ever increasing demand for personal/consumer communication applications.

Dual-band bandpass filters can be divided into two categories. Category I is where the frequency separation between the two bands is small and category II is where the frequency separation between the two bands is large. Dual-band bandpass filters in category I are particularly useful for rejecting unwanted frequency spectrum that falls in between a wanted band of the frequency spectrum. Whereas dual-band bandpass filters in category II are useful for communication system that employs multiple frequency spectrum bands, e.g. Wireless LAN at 2.4 GHz and 5.2 GHz. For category I application, conventionally, it is achieved by cascading a bandpass filter with a bandstop filter [1]. With the advancement in the filter design theories, a dual-band bandpass filter can be achieved by placing transmission zeros into the passband of a wider-bandwidth bandpass filter to achieve a stopband within the passband. This type of dual-band bandpass filter is achieved by cross-coupling arrangement between synchronously tuned resonators. Although theoretically there is no reason why a cross-coupled dual-band filter cannot be achieved in category II, in practice the coupling strength requirements are normally too strong to be realized. Category II dual-band bandpass filters are normally achieved by employing the harmonic of the fundamental resonator mode [2], using quarter-wavelength admittance inverters between resonators [3] instead of electromagnetic coupling or even using cross-coupled asynchronously tuned resonators [4].

In this paper, the category I dual-band filter will be presented based on coupling of synchronously tuned resonators. The bandwidth of the two individual bandpass filter is 10 MHz with a fractional bandwidth of approximately 0.5%. The fractional bandwidth of the dual-band is 1.6%, i.e. $(f_{o,BPU} - f_{o,BPL})/f_o$ [3]. The circuit model and electromagnetic simulations together with cryogenic measurement will be presented.

II. Dual-Band Filter Design

The dual-band filter presented in this paper consists of 8 resonators. The filter will have 8 poles where 4 poles are located on each passband. In addition, the filter will also exhibit 4 transmission zeros, a pair of transmission zero for each passband.

Fig. 1 shows the configuration of all the resonators and the coupling layout of the dual-band bandpass filter. The dual-band characteristic is achieved by having weaker coupling strength between the resonators 4 and 5 in comparison to the coupling strength between the resonators 3 and 6. In a single band bandpass filter, the coupling between the resonators 4 and 5 must be stronger than the coupling between the resonators 3 and 6.

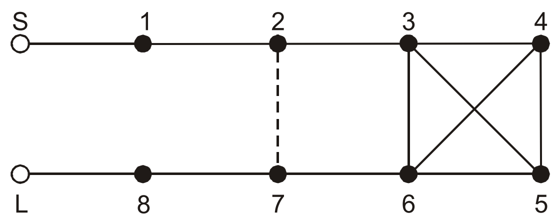

Fig. 1. Dual-band bandpass filter resonators and the coupling configuration (coupling: slash line is 180° phase different compared to solid line and black dot = resonator)

The specification of the designed dual-band bandpass filter is

Center frequency, f_o:	1975.5 MHz
Center frequency of lower passband, $f_{o,BPL}$:	1960 MHz
Center frequency of upper passband, $f_{o,BPU}$:	1991 MHz
Bandwidth of lower passband, BW_L:	10 MHz
Bandwidth of upper passband, BW_U:	10 MHz

A circuit model of the dual-band filter is formulated and simulated using Agilent Advanced Design Systems (ADS). All the 8 resonators are modeled using parallel inductor, L, and capacitor, C, which has a value of 5.77×10^{-4} nH and 1.1241×10^{4} pF, respectively. The coupling between resonators is modeled using admittance inverters (J-inverters) in the form of PI-capacitors [5, 6]. The J-inverter values are

$J_{12} = J_{78} = 2.396$	$J_{36} = 0.650$
$J_{23} = J_{67} = 1.142$	$J_{27} = -0.148$
$J_{34} = J_{56} = 2.028$	$J_{35} = J_{46} = 0.006$
$J_{45} = 0.392$	$J_{01} = J_{89} = 1.239$

The corresponding coupling coefficients can be determined using Eqn. (5) in [5] and external quality factor can be determined using Eqn. (1) and the values are

$M_{12} = M_{78} = 0.01717$	$M_{36} = 0.00466$
$M_{23} = M_{67} = 0.00818$	$M_{27} = -0.00106$
$M_{34} = M_{56} = 0.01454$	$M_{45} = 0.00281$
$M_{35} = M_{46} = 0.000045$	$Q_{ext} = 113$

$$Q_{ext} = \frac{\omega_o C}{J_{m,m+1}} \quad \text{where } m = 0 \text{ or } n \text{ (the order of the filter)} \qquad (1)$$

III. Microstrip Design

The microstrip dual-band bandpass filter uses folded hairpin resonator topology, which is shown in Fig. 2, as the building block. From the coupling layout shown in Fig. 1, an in-phase cross coupling is required, i.e. M_{36} and M_{45} are in-phase. To achieve in-phase cross coupling for microstrip resonators, with at least one symmetrical axis (shown in Fig. 3) the resonators have to be arranged in a similar fashion as those shown in Fig. 4.

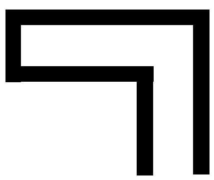

Fig. 2. Folder hairpin resonator.

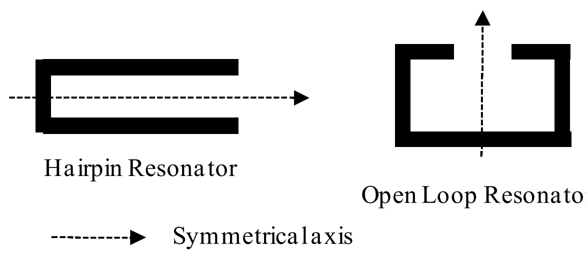

Fig. 3. Microstrip resonator with at least one symmetrical axis.

With close inspection, one will notice that unwanted couplings between the resonators 3 and 5 and the resonators 4 and 6 will exist in that arrangement. In comparison to the arrangement for out-of-phase cross coupling, which is often used to introduce a pair of transmission zeros in cascaded quadruplet filters [6], the unwanted coupling between the resonators 3 and 5 and the resonators 4 and 6 are much weaker. This can be explained based on mixed coupling. The coupling structure between the resonators 3 and 5 in an in-phase cross coupling arrangement, will exhibit a type-I mixed coupling, where the electric and magnetic couplings enhance each other [5]. Whereas in out-of-phase cross-coupling arrangement, the coupling between the resonators 3 and 5 and the resonators 4 and 6 will exhibit type-II mixed coupling where the electric and magnetic couplings cancelling each other out [6]. As a result, for the same coupling distance, the coupling between the resonators 3 and 5 and the resonators 4 and 6 are much stronger in an in-phase cross-coupling structure compared to an out-of-phase cross-coupling structure. Therefore, the unwanted coupling has a much stronger effect in distorting the filter characteristic in an in-phase cross-coupling structure.

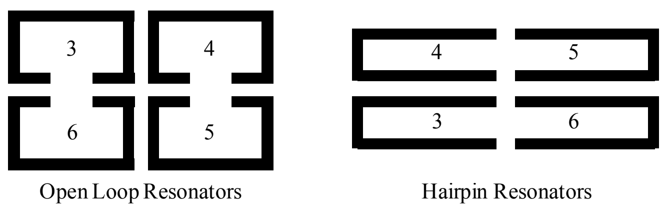

Fig. 4. Arrangement of in-phase cross coupling (M_{36} and M_{45} are in-phase) for resonator with one symmetrical axis.

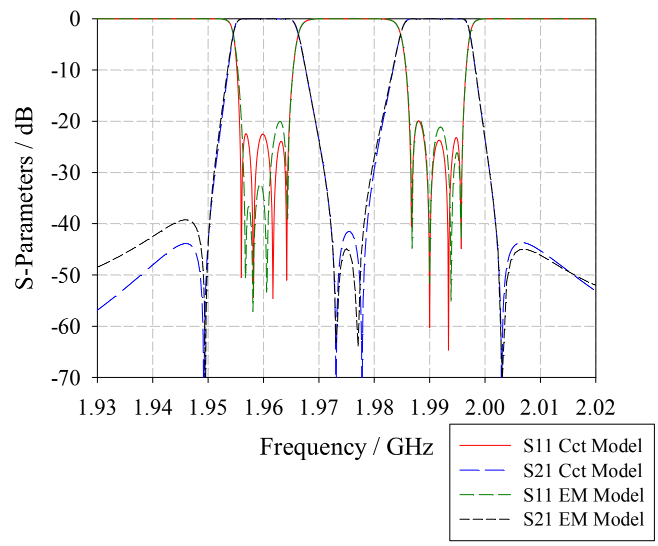

Fig. 5. Comparison of circuit model and EM simulation results

In order to reduce the unwanted cross-coupling, the folded hairpin resonator is introduced. By removing all the symmetries in the resonator structure, the resonators 3 and 5 and the resonators 4 and 6 can be placed further away in an in-phase cross-coupling arrangement. However, in a planar structure, coupling between resonators is always present no matter how far apart they are placed except in the type-II mixed coupling when the electric coupling and magnetic coupling is equal. In this design, the weak coupling of the resonators 3 and 5 and the resonators 4 and 6 are incorporated in the design.

The microstrip dual-band bandpass filter is simulated using Momentum of Agilent Advanced Design Systems. The simulation results are given in Fig. 5. In Fig. 5, the circuit model simulation results are also presented. The EM simulation results show a good agreement with the circuit model simulation results.

IV. Circuit Fabrication

The high temperature superconductor (HTS) dual-band bandpass filter is fabricated using photolithographic process onto a single crystal Magnesium Oxide (MgO) substrate with a thin film of Yttrium Barium Copper Oxide (YBCO) on both sides. The YBCO films have a thickness of 600 nm with T_c of 87.7 K and J_c of 2.4 MA/cm^2. The MgO substrate has a thickness on 0.508 mm with dielectric constant of 9.8 and loss tangent in the region of 10^{-6}.

The layout of the 8 pole dual-band bandpass filter (4 poles on each bandpass) with 4 transmission zeros is shown in Fig. 6. The linewidth of the microstrip is 0.5mm which is designed for 50 Ω.

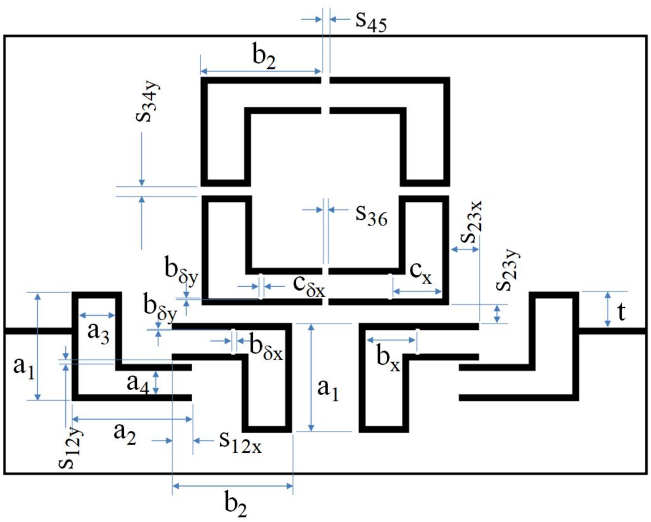

Fig. 6. Dual-band bandpass filter layout

The dimensions of the filter layout parameters corresponding to Fig. 6 are given in Table I. All the dimensions given in Table I are in mm.

The fabricated HTS circuit is mounted on a gold plated titanium carrier. Titanium is used because of its thermal expansion coefficient which is relatively close to the thermal expansion coefficient of MgO. This is important to ensure that the MgO will not crack due different expansion rate when cooling from 300 K down to 60 K. The titanium carrier is then mounted on a brass housing fixed with K-connectors. Sliding contacts are used for connecting the K-connectors to the HTS microstrip input and output feed lines. Fig. 7 shows a photograph of the assembled HTS dual-band bandpass filter with its lid opened.

TABLE I
Summary of Circuit Layout Parameters

a_1	a_2	a_3	a_4	b_2	b_x	$b_{\delta x}$
8.3	9.099	2.8	2.8	9.112	3.8	0.32
c_x	$c_{\delta x}$	s_{12x}	s_{12y}	s_{23x}	s_{23y}	s_{34y}
3.8	0.3	0.3	1.5311	2.287	1.3805	0.6908
s_{45}	s_{36}	t				
0.648	0.4936	2.7349				

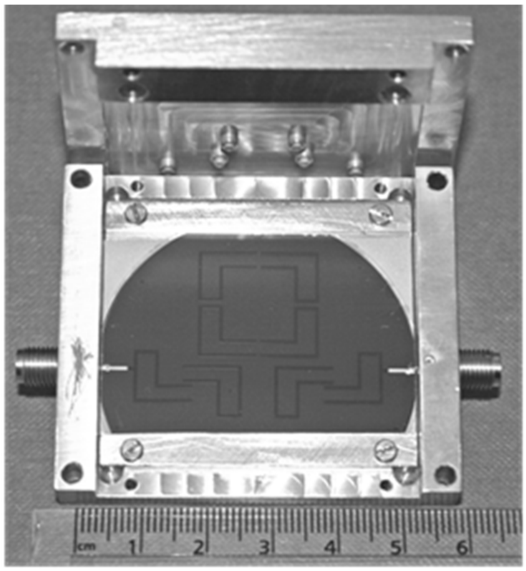

Fig. 7. Photograph of the assembled HTS dual-band passband filter

V. Experimental Results

The assembled HTS dual-band bandpass filter is mounted onto the cold head of Sterling Cooler. The filter is cooled down to 60 K and the filter response is measured. Fig. 8 shows the filter response without any tuning performed. The measured results show good agreement with the EM simulated results. There is a shift of approximately 2.3 MHz upward in the frequency response of the measured filter. This shift can be corrected/tuned using mechanical tuning screws [7]. However, this was not performed in this experiment. The measured ripple is also slightly greater than the simulated. This is mainly due to fabrication tolerance and variation of substrate thickness across the circuit.

The measured insertion loss shows gain of approximately 0.5 dB. This is due to the calibration being performed at room temperature while the measurement was performed at 60 K. Therefore, the reference point of the calibration has shifted. Fig. 9 shows a close up of the passband ripple. At approximately 1.953 GHz, the $|S_{11}|$ is measured at approximately 0.23 dB which correspond to a transmission zero at the $|S_{21}|$. If the calibration was performed at 60 K, the $|S_{11}|$ of this transmission zero is approximately at 0 dB. Therefore, it is a safe hypothesis to assume that the 0 dB reference is very close to the return loss at 1.953 GHz. Using that as reference, the minimum filter passband insertion loss is estimated as 0.18 dB. Fig. 9 shows a wideband measurement of the filter. There is no spurious mode measured between 1 GHz to 3 GHz spectrum as shown in Fig. 10.

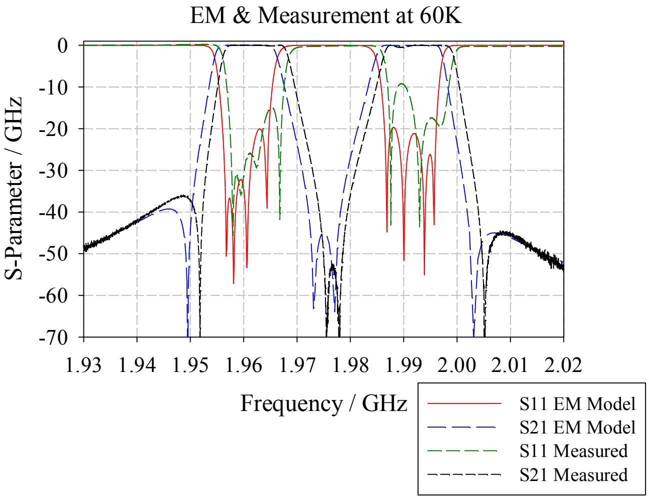

Fig. 8. Comparison of EM simulation and measurement results at 60 K

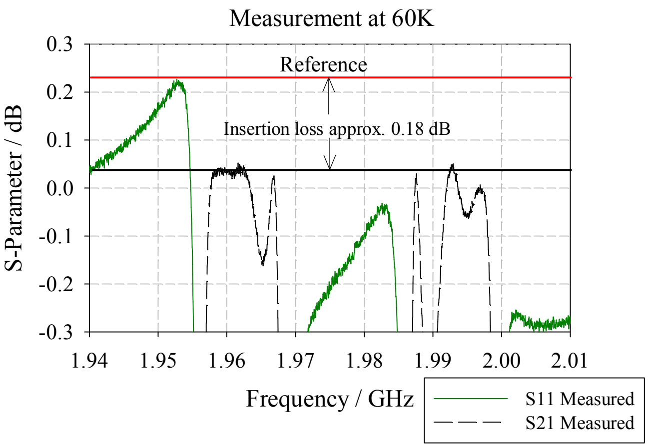

Fig. 9. Close-up response of the passband ripple at 60 K

VI. Conclusion

The simulation and experimental results of an 8 pole HTS dual-band bandpass filter have been presented. The experimental results are in good agreement with the design. Good isolation between the two passband has also been achieved in the experimental results. However, further improvement can be achieved by fine tuning the resonators centre frequencies. This can be done by using mechanical tuning screws which are mounted on the box lid. The loss of the filter is very small. The minimum passband insertion loss is estimated at approximately 0.18 dB.

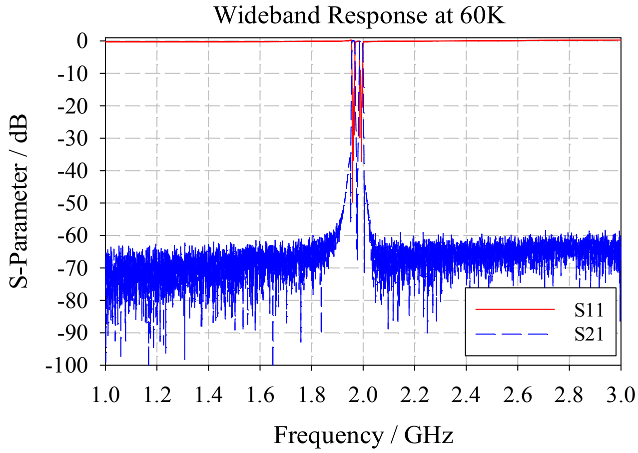

Fig. 10. Wideband measurement of the HTS filter at 60 K

Acknowledgement

This work was funded under EPSRC Portfolio grant – GR/S60471/01. The authors would like to Clifford Ansell and Donna M. Holdom from the University of Birmingham for their technical assistance.

References

[1] L. -C. Tsai and C. –W. Hsue, "Dual-Band Bandpass Filters Using Equal-Length Coupled-Serial-Shunted Lines and Z-Transform Technique," *IEEE Trans. Microwave, Theory & Tech.*, vol. 52, no. 4, pp. 1111-1117, April 2004.

[2] S. -F. Cheng, Y. -L. Jeng, and J. -L. Chen, "Dual-Band Step-Impedance Bandpass Filter for Multimode Wireless LANs," *Electronics Letters*, vol. 40, no. 1, pp. 38-39, 2004.

[3] X. Guan, Z. Ma, P. Cai, Y. Kobayashi, T. Anada and G. Hagiware, "Synthesis of Dual-Band Bandpass Filters Using Successive Frequency Transformation and Circuit Conversions," IEEE *Microwave & Wireless Components letters*, vol. 16, no. 3, 2006.

[4] J. –T. Kuo, H. –S. Cheng, "Design of Quasi-Elliptic Function Filters With a Dual-Passband Response," *IEEE Microwave & Wireless Components Letters*, vol. 14, no. 10, 2004.

[5] K. S. K. Yeo, M. J. Lancaster and J. -S. Hong, "The Design of Microstrip Six-Pole Quasi-Elliptic Filter with Linear Phase Response Using Extracted-Pole Technique," *IEEE Trans. Microwave Theory & Tech.*, vol. 49, no. 2, pp 321-327, 2002.

[6] J. -S. Hong and M. J. Lancaster, "Couplings of Microstrip Square Open-Loop Resonators for Cross-Coupled Planar Microwave Filters," *IEEE Trans. Microwave Theory & Tech.*, vol. 44, no. 12, pp. 2099-2108, 1996.

[7] J.-S Hong, M. J. Lancaster, D. Jedamzik and R. B. Greed, "On the Development of Superconducting Microstrip Filters for Mobile Communications Applications", *IEEE Trans. Microwave Theory & Tech.*, vol. 47, no. 9, pp. 1656-1663, 1999.